

Proton skins, neutron skins, and proton radii of mirror nuclei.

Francesca Sammarruca

Physics Department, University of Idaho, Moscow, ID 83844-0903, U.S.A.

(Dated: July 19, 2021)

We present predictions for proton skins based on isospin-asymmetric equations of state derived microscopically from high-precision chiral few-nucleon interactions. Moreover, we investigate the relation between the neutron skin of a nucleus and the difference between the proton radii of the corresponding mirror nuclei.

I. INTRODUCTION

It is well known that the available information on neutron radii and neutron skins is scarce and carry considerable uncertainty, see, for instance, Ref. [1] and references therein for a summary of empirical constraints, particularly on the skin of ^{208}Pb , obtained from a variety of measurements. Although future experiments [2, 3] are anticipated which should provide reliable information on the weak charge density in ^{208}Pb and ^{48}Ca , the identification of other “observables” whose knowledge may give complementary information on neutron skins would be most welcome.

Naturally, the possibility of obtaining reliable values for neutron or proton skins is hindered by similar limitations, as both proton and neutron radii must be known to extract either skin. And while charge densities, particularly for stable isotopes, have been measured with great accuracy, the same cannot be said for the weak charge density.

An issue of current interest is whether information on the neutron skin can be obtained through the knowledge of proton radii alone, specifically those of mirror nuclei. In particular, the difference between the charge radii of mirror nuclei in relation to the slope of the symmetry energy, and, in turn, to the neutron skin, was investigated in Ref. [4]. As done in the past by the same author [5], correlations between neutron skins and the slope of the symmetry energy are deduced using large sets of phenomenological interactions, such as the numerous parametrizations of the Skyrme interactions. In Ref. [4], using similar methods and 48 Skyrme functionals, a proportionality relation was found between the difference in the charge radii of mirror nuclei and the slope of the symmetry energy. This was echoed in Ref. [6] using a set of relativistic energy density functionals.

Although phenomenological analyses are a useful exploratory tool to gain some preliminary insight into sensitivities and interdependences among nuclear properties, only through microscopic predictions can we understand a result in terms of the physical input. The purpose of this work is twofold. First, we present proton skin predictions and observe general patterns within isotopic chains, comparing with data when available. Second, we wish to explore, from the microscopic point of view in contrast to the phenomenological one, the relation between the neutron skin of a nucleus, on the one hand, and the difference between the proton radii of the mirror pair with the same mass, on the other. To avoid confusion, we underline that this analysis will not be done by varying parameters in a family of models (not an option consistent with the microscopic approach). Instead, we shall investigate our predicted relation between the quantities defined above for a variety of (realistic) mirror pairs. We will pay particular attention to proton radii of mirror nuclei specifically in the mass range $A \approx 48 - 54$. At this time, the determination of proton radii of neutron-deficient isotopes such as, for instance, the “mirror” of $^{54}_{26}\text{Fe}$ is an enormous experimental challenge, which may be met in the future at radioactive beam facilities.

Our predictions are based on microscopic high-precision nuclear interactions derived from chiral Effective Field Theory (EFT) [7]. In this way, we hope to provide useful microscopic input to be taken into account in future analyses.

This paper is organized as follows. In the next section, we give a short review of the theoretical tools and the calculation of the neutron and proton skins. We then proceed to proton skin predictions (Sect. III) and, more specifically, those of some mirror pairs in selected mass ranges (Sect. IV). A brief summary and our conclusions are contained in Sect. V.

II. BRIEF REVIEW OF THE THEORETICAL INPUT

A. The few-nucleon forces

In recent years, chiral EFT has evolved into the authoritative approach to construct nuclear two- and many-body forces in a systematic and essentially model-independent manner [7, 8]. Nucleon-nucleon (NN) potentials are available from leading order (LO, zeroth order) to N^3LO (fourth order) [7–11], with the latter reproducing NN data at the high precision level. More recently, NN chiral potentials at N^4LO have also been developed [12, 13].

A large number of applications of chiral NN potentials (usually up to N³LO) together with chiral three-nucleon forces (3NF) (generally just at N²LO) have been conducted. A fairly extensive, although not exhaustive list is given in Refs. [14–36].

We apply the microscopic equations of state (EoS) of symmetric nuclear matter and the ones of pure neutron matter as derived in Ref. [36]. The derivation is based on high-precision chiral NN potentials at next-to-next-to-next-to-leading order (N³LO) of chiral perturbation theory [7, 10]. The leading 3NF, which is treated as an effective density-dependent force [37], is included.

B. Additional tools

This section provides a very brief summary of previously developed tools to obtain nuclear properties from the infinite-matter EoS [38]. Within the spirit of a liquid droplet model, the energy of a nucleus is written in terms of a volume, a surface, and a Coulomb term as

$$E(Z, A) = \int d^3r e(\rho, \alpha) \rho(r) + \int d^3r f_0 |\nabla \rho|^2 + \frac{e^2}{4\pi\epsilon_0} (4\pi)^2 \int_0^\infty dr' r' \rho_p(r') \int_0^{r'} dr r^2 \rho_p(r). \quad (1)$$

In the above equation, ρ is the total nucleon density, given by $\rho_n + \rho_p$, with ρ_n and ρ_p the neutron and proton densities, respectively. α is the neutron asymmetry parameter, $\alpha = \rho_I / \rho$, where the isovector density ρ_I is given by $(\rho_n - \rho_p)$. $e(\rho, \alpha)$ is the energy per particle in isospin-asymmetric nuclear matter, written as

$$e(\rho, \alpha) = e(\rho, 0) + e_{sym}(\rho) \alpha^2, \quad (2)$$

with $e_{sym}(\rho)$ the symmetry energy. The density functions for protons and neutrons are obtained by minimizing the value of the energy, Eq. (1), with respect to the parameters of Thomas-Fermi distributions,

$$\rho_i(r) = \frac{\rho_0}{1 + e^{(r-a_i)/c_i}}, \quad (3)$$

with $i = n, p$. The radius and the diffuseness, a_i and c_i , respectively, are extracted by minimization of the energy while ρ_0 is obtained by normalizing the proton(neutron) distribution to $Z(N)$. The neutron and proton skins are defined in the usual way,

$$S_n = R_n - R_p, \quad (4)$$

and

$$S_p = R_p - R_n, \quad (5)$$

respectively, where R_n and R_p are the *r.m.s.* radii of the neutron and proton density distributions,

$$R_i = \left(\frac{4\pi}{T} \int_0^\infty \rho_i(r) r^4 dr \right)^{1/2}, \quad (6)$$

and $T = N$ or Z . We stress that the above method has the advantage of allowing for a very direct connection between the EoS and the properties of finite nuclei. It was used in Ref. [38] in conjunction with meson-theoretic potentials and found to yield realistic predictions for binding energies and charge radii. The constant f_0 in the surface term is typically obtained from fits to β -stable nuclei and determined to be about 60-70 MeV fm⁵ [39]. How this uncertainty impacts the corresponding predictions was discussed in Ref. [1] and will be taken into account in the present calculations.

III. PREDICTIONS FOR PROTON SKINS

In Table I, we display proton skin predictions for some isotopic chains. The EoS used for these predictions is based upon N³LO two-nucleon forces (2NF) plus the leading 3NF. The estimated theoretical errors include uncertainties due to variations of the cutoff in the range 450-500 MeV as well as an error (added in quadrature) to account for the uncertainty originating from the method we use to calculate the skins [1]. The latter error is in the order of ± 0.01 fm, but varies with the size of the skin.

As a general feature, we observe that the proton skins can be quite large. In fact, the *neutron* skins of the corresponding (neutron-rich) mirror nuclei are smaller. This fact is demonstrated in Table II, where we show, for

TABLE I: Proton skins, S_p , for $Z=10, 11, 17$, and 18 isotopic chains. See text for more details.

Z	A	S_p (fm)
10	16	0.422 ± 0.022
	17	0.287 ± 0.014
	18	0.186 ± 0.012
	19	0.103 ± 0.006
	20	0.032 ± 0.006
11	18	0.373 ± 0.020
	19	0.260 ± 0.012
	20	0.172 ± 0.012
	21	0.098 ± 0.006
	22	0.034 ± 0.006
17	31	0.180 ± 0.012
	32	0.131 ± 0.011
	33	0.086 ± 0.008
	34	0.045 ± 0.007
18	29	0.439 ± 0.025
	30	0.352 ± 0.019
	31	0.283 ± 0.014
	32	0.225 ± 0.013
	33	0.174 ± 0.013
	34	0.127 ± 0.012
	35	0.085 ± 0.008
	36	0.046 ± 0.007

the most neutron-deficient isotope in each chain, the proton skin together with the neutron skin of the corresponding mirror nucleus.

Some data on proton skins can be found in Refs. [48–51]. In Ref. [49], the existence of neutron and proton skins in β -unstable neutron- or proton-rich Na and Mg isotopes is discussed based on measurements of the interaction cross sections of these isotopes incident on a carbon target around 950 A MeV. In Ref. [50], proton skin thickness for isotopes $^{32-40}\text{Ar}$ were deduced from the interaction cross sections of $^{31-40}\text{Ar}$ and $^{31-37}\text{Cl}$ on carbon targets. The obtained matter radii were combined with measured charge radii for Argon isotopes to obtain skin thicknesses.

In Fig. 1, we show our predictions for the proton skins of Argon isotopes in comparison with data deduced from experiments as described in Ref. [50]. Keeping in mind the large experimental errors, the trend of the empirical information is described reasonably well by our predictions, where the proton skin decreases essentially monotonically with increasing number of neutrons in a given isotopic chain.

IV. MIRROR NUCLEI

A. Symmetry of mirror nuclei

Assuming perfect charge symmetry, one has, in mirror nuclei,

$$R_n(Z, N) = R_p(N, Z), \quad (7)$$

a relation which we have verified to be exactly satisfied when Coulomb contributions and other charge-dependent effects are turned off. Applying the definition of the neutron skin,

$$S_n(Z, N) = R_n(Z, N) - R_p(Z, N), \quad (8)$$

we can then immediately conclude from Eq. (7) that

$$S_n(Z, N) = R_n(Z, N) - R_p(Z, N) = R_p(N, Z) - R_p(Z, N) \equiv \Delta R_p. \quad (9)$$

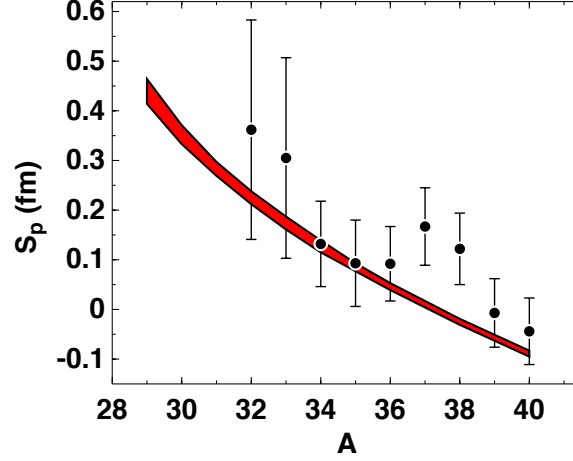


FIG. 1: (Color online) Predicted proton skins of Argon isotopes as a function of the mass number, A . The data points are from Ref. [50].

TABLE II: Predicted proton skins, S_p , for the given Z and A and neutron skins, S_n^{mirr} , of the corresponding mirror nuclei.

Z	A	S_p (fm)	S_n^{mirr} (fm)
10	16	0.422 ± 0.022	0.333 ± 0.016
11	18	0.373 ± 0.020	0.286 ± 0.011
17	31	0.180 ± 0.012	0.091 ± 0.006
18	29	0.439 ± 0.025	0.310 ± 0.010

Namely, the neutron skin of nucleus (Z, N) would be *equal* to the difference between the proton radii of the mirror pair in the presence of perfect charge symmetry. If charge radii could be measured accurately for mirror pairs in the desired mass range, then the neutron skin of the (Z, N) nucleus could be obtained from Eq. (9) after theoretical considerations to account for charge effects. Thus, this could be an alternative, although perhaps equally challenging from the experimental side, to the anticipated parity-violating experiments [4].

TABLE III: Proton skins, S_p , in the mass range 48-54.

Z	A	S_p (fm)
20	48	-0.181 ± 0.010
28	48	0.316 ± 0.021
22	50	-0.112 ± 0.010
28	50	0.238 ± 0.016
24	52	-0.048 ± 0.007
28	52	0.169 ± 0.013
26	54	0.008 ± 0.006
28	54	0.112 ± 0.013

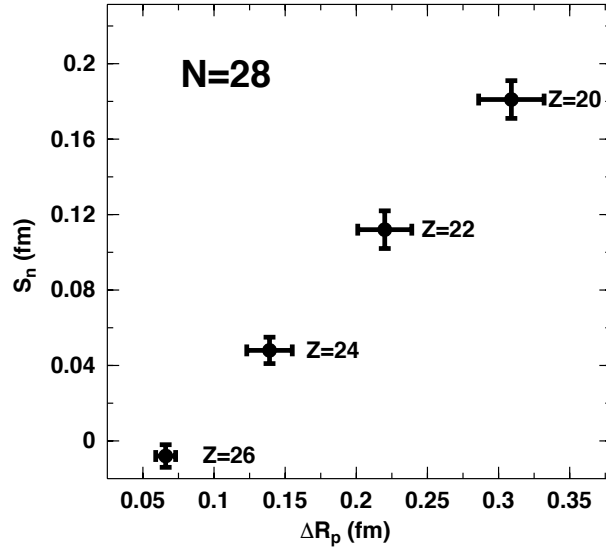


FIG. 2: Graphical representation of Table IV.

B. Radii and skins of mirror nuclei for $A \approx 50$

We now move to a specific range within medium mass nuclei, namely $A \approx 48 - 54$. This choice can be motivated by the vicinity to ^{48}Ca , whose neutron skin has already been and is likely to be in the future the object of several investigations, both theoretical and experimental. At the same time, the need to consider mirror pairs limits the spectrum of realistic possibilities.

Table IV displays the neutron skin of the neutron-rich isotones from Table III in relation to ΔR_p as defined in Eq. (9), with and without Coulomb effects. (Note that the latter case will not be addressed again and is shown here only for numerical verification, since the two items appearing in parentheses in Table IV are expected to be exactly equal to each other on grounds of elementary nuclear physics.)

Increasing ΔR_p implies increasing the neutron skin, as one might reasonably expect unless Coulomb effects were to reverse the relation in Eq. (9). Note, though, that quantitatively speaking Coulomb effects are significant.

Next we wish to explore the relation between ΔR_p and $S_n(Z, N)$ for other chains. In particular, we wish to investigate if and how such relation differs, quantitatively, among chains with different masses. For that purpose, we consider in Table V and VI two *isotopic* chains, one of them in a mass range considerably different than the one studied in Table IV. A visual representation of Tables IV, V, and VI is provided in Figs. 2, 3, and 4.

The first observation is that, for similar values of ΔR_p , the corresponding values of $S_n(Z, N)$ are approximately the same, regardless Z and N . Also, in all three cases the relation is clearly linear. We stress again that the results shown in Figs. 2, 3, and 4 are fundamentally distinct from the correlations discussed in Ref. [4]. The latter are obtained varying the parameters of Skyrme models (each model constrained to produce a chosen value of the neutron skin in ^{208}Pb) for a fixed mirror pair. Here, we explore to which extent our microscopic EoS yields, within theoretical uncertainties, a unique relation between S_n and ΔR_p .

The parameters of our predicted linear relation,

$$S_n = a(\Delta R_p) + b, \quad (10)$$

based upon the three cases shown in Figs. 2, 3, and 4, can be summarized as

$$a = 0.78 \pm 0.05 \quad b = -0.044 \pm 0.016. \quad (11)$$

By means of Eqs. (10-11), a measurement of ΔR_p can then be promptly related to the neutron skin of the neutron-rich nucleus in the mirror pair.

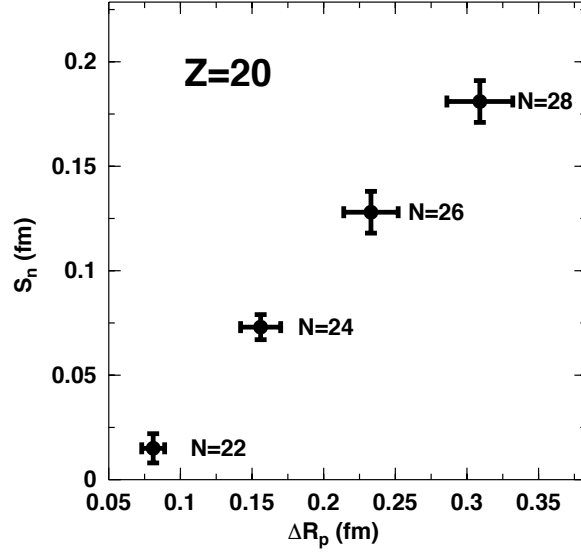


FIG. 3: Graphical representation of Table V.

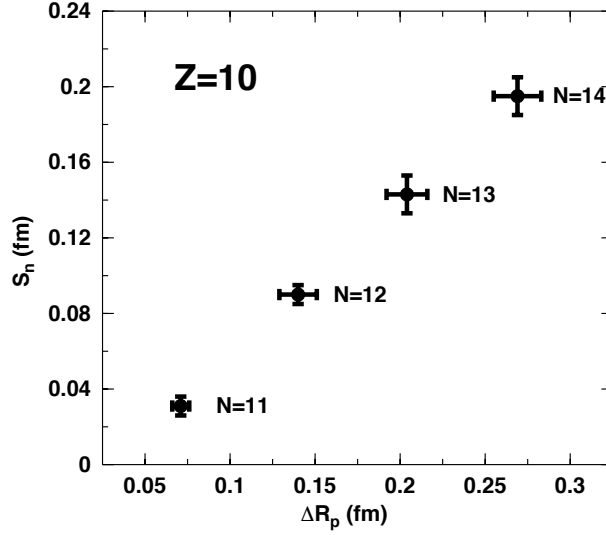


FIG. 4: Graphical representation of Table VI.

Microscopic predictions do, of course, differ from one another. Although EFT should, in principle, be a model-independent approach, even EFT-based predictions can differ between them, depending, for instance, on the details of the input forces (e.g. cutoff) and the chosen many-body method. Moreover, the microscopically-predicted relations between two quantities or observables are not necessarily located on one of the Skyrme models correlations. Here, we suggest that analyses such as the present one, combined with other microscopic predictions, are the best way to provide a global relation between the “observables” being studied (as well as their relation to the density dependence of the symmetry energy), accompanied by a meaningful theoretical uncertainty.

TABLE IV: Relation between the neutron skin of nucleus (Z, N) , $S_n(Z, N)$, and ΔR_p of the corresponding mirror pair for the isotone chain $N=28$. The values in paranthesis are the results without Coulomb contribution (as a verification).

Z	N	$S_n(Z, N)(\text{fm})$	$\Delta R_p(\text{fm})$
20	28	0.181 ± 0.010 (0.229)	0.309 ± 0.023 (0.229)
22	28	0.112 ± 0.010 (0.162)	0.220 ± 0.019 (0.162)
24	28	0.048 ± 0.007 (0.103)	0.139 ± 0.016 (0.103)
26	28	-0.008 ± 0.006 (0.049)	0.066 ± 0.007 (0.049)

TABLE V: Relation between the neutron skin of nucleus (Z, N) , $S_n(Z, N)$, and ΔR_p for the isotope chain $Z=20$.

Z	N	$S_n(Z, N)(\text{fm})$	$\Delta R_p(\text{fm})$
20	22	0.015 ± 0.007	0.081 ± 0.008
20	24	0.073 ± 0.006	0.156 ± 0.014
20	26	0.128 ± 0.010	0.233 ± 0.019
20	28	0.181 ± 0.010	0.309 ± 0.023

V. SUMMARY AND CONCLUSIONS

Microscopic predictions of the EoS for isospin-asymmetric nuclear matter have been applied to obtain proton and neutron skins of selected chains of nuclei. The calculations of the EoS are based on high-precision chiral forces.

First, we presented proton skin predictions for a few isotopic chains to observe some of their general fetures, particularly in comparison with neutron skins. We find that they are generally large, larger than neutron skins for comparable values of proton-neutron asymmetry. Our predictions compare well with available empirical information.

We then moved the focus on to mirror nuclei in a specific mass range ($A \approx 48-54$). At this point we took the opportunity to make some comments about and highlight differences with recent studies [4, 6] which have addressed those nuclei.

Using our microscopic predictions and their uncertainties, we constructed a correlation between the skin of a neutron-rich nucleus and the difference between the proton radii of the corresponding mirror pair. We discussed the meaning and significance of such correlation in contrast to those characteristic of phenomenological studies. Given the *ab initio* nature of the EoS, we are in the position of exploring, for instance, the contribution of 3NF to the predictions, the impact of higher chiral orders, and the order-by-order pattern of the chiral perturbation series.

We conclude by highlighting the importance of taking into account microscopic predictions as a guide towards the planning of future measurements.

Acknowledgments

This work was supported by the U.S. Department of Energy, Office of Science, Office of Basic Energy Sciences, under Award Number DE-FG02-03ER41270.

[1] F. Sammarruca, Phys. Rev. C **94**, 054317 (2016).

TABLE VI: Relation between the neutron skin of nucleus (Z, N) , $S_n(Z, N)$, and ΔR_p for the isotope chain $Z=10$.

Z	N	$S_n(Z, N)(\text{fm})$	$\Delta R_p(\text{fm})$
10	11	0.031 ± 0.005	0.071 ± 0.005
10	12	0.090 ± 0.005	0.140 ± 0.011
10	13	0.143 ± 0.010	0.204 ± 0.012
10	14	0.195 ± 0.010	0.269 ± 0.014

- [2] S. Abrahamyan *et al.* (PREX Collaboration), Phys. Rev. Lett. **108**, 112502 (2012).
- [3] J. Mammei *et al.*, <http://hallaweb.jlab.org/parity/prex/c-rex/c-rex.pdf>.
- [4] B.A. Brown, Phys. Rev. Lett. **119**, 122502 (2017).
- [5] B.A. Brown, Phys. Rev. Lett. **85**, 5296 (2000).
- [6] Junjie Yang and J. Piekarewicz, arXiv:1709.10182 [nucl-th].
- [7] R. Machleidt and D.R. Entem, Physics Report **503**, 1 (2011).
- [8] E. Epelbaum, H.-W. Hammer, and U.-G. Meissner, Rev. Mod. Phys. **81**, 1773 (2009).
- [9] E. Marji, A. Canul, Q. MacPherson, R. Winzer, Ch. Zeoli, D.R. Entem, and R. Machleidt, Phys. Rev. C **88**, 054002 (2013).
- [10] D.R. Entem and R. Machleidt, Phys. Rev. C **68**, 041001 (2003).
- [11] E. Epelbaum, W. Glöckle, and U.-G. Meissner, Nucl. Phys. A **747**, 362 (2005).
- [12] E. Epelbaum, H. Krebs, and U.-G. Meissner, Phys. Rev. Lett. **115**, 122301 (2015).
- [13] D.R. Entem, R. Machleidt, and Y. Nosyk, Phys. Rev. C **96**, 024004 (2017).
- [14] B.R. Barrett, P. Navrátil, and J.P. Vary, Prog. Part. Nucl. Phys. **69**, 131 (2013).
- [15] S. Binder, J. Langhammer, A. Calci, and R. Roth, Phys. Lett. B **736**, 119 (2014).
- [16] S. Binder, J. Langhammer, A. Calci, P. Navrátil, and R. Roth, Phys. Rev. C **87**, 021303 (2013).
- [17] G. Hagen, T. Papenbrock, D.J. Dean, and M. Hjorth-Jensen, Phys. Rev. Lett. **101**, 092502 (2008).
- [18] H. Hergert, S. Bogner, T. Morris, A. Schwenk, and K. Tsukiyama, Phys. Rep. **621**, 165 (2016).
- [19] S.R. Stroberg, H. Hergert, J.D. Holt, S.K. Bogner, and A. Schwenk, Phys. Rev. C **93**, 051301 (2016).
- [20] J. Simonis, K. Hebeler, J.D. Holt, J. Menendez, and A. Schwenk, Phys. Rev. C **93**, 011302 (2016).
- [21] K. Hebeler, J. Holt, J. Menendez, and A. Schwenk, Annual Review of Nuclear and Particle Science **65**, 457 (2015).
- [22] A. Ekström *et al.*, Phys. Rev. C **91**, 051301 (2015).
- [23] T.A. Lähde, E. Epelbaum, H. Krebs, D. Lee, U.-G. Meissner, and G. Rupak, Phys. Lett. B **732**, 110 (2014).
- [24] L. Coraggio, J.W. Holt, N. Itaco, R. Machleidt, L.E. Marcucci, and F. Sammarruca, Phys. Rev. C **89**, 044321 (2014).
- [25] A. Cipollone, C. Barbieri, and P. Navrátil, Phys. Rev. Lett. **111**, 062501 (2013).
- [26] V. Somá, A. Cipollone, C. Barbieri, P. Navrátil, and T. Duguet, Phys. Rev. C **89**, 061301 (2014).
- [27] A. Cipollone, C. Barbieri, and P. Navrátil, Phys. Rev. C **92**, 014306 (2015).
- [28] A. Carbone, A. Rios, and A. Polls, Phys. Rev. C **88**, 044302 (2013).
- [29] H. Hergert, S. Binder, A. Calci, J. Langhammer, and R. Roth, Phys. Rev. Lett. **110**, 242501 (2013).
- [30] S. Fiorilla, N. Kaiser, and W. Weise, Nucl. Phys. A **880**, 65 (2012).
- [31] S. Bogner, R. Furnstahl, H. Hergert, M. Kortelainen, P. Maris, *et al.*, Phys. Rev. C **84**, 044306 (2011).
- [32] P. Navrátil, R. Roth, and S. Quaglioni, Phys. Rev. C **82**, 034609 (2010).
- [33] V. Lapoux, V. Somá, C. Barbieri, H. Hergert, J.D. Holt, and S.R. Stroberg, Phys. Rev. Lett. **117**, 05250 (2016).
- [34] G. Hagen *et al.*, Nature Physics **12**, 186 (2016).
- [35] T. Krüger, I. Tews, K. Hebeler, and A. Schwenk, Phys. Rev. C **88**, 025802 (2013).
- [36] F. Sammarruca, L. Coraggio, J.W. Holt, N. Itaco, R. Machleidt, and L.E. Marcucci, Phys. Rev. C **91**, 054311 (2015).
- [37] J.W. Holt, N. Kaiser, and W. Weise, Phys. Rev. C **79**, 054331 (2009); Phys. Rev. C **81**, 024002 (2010).
- [38] D. Alonso and F. Sammarruca, Phys. Rev. C **68**, 054305 (2003).
- [39] K. Oyamatsu, Kei Iida, and Hiroyuki Koura, Phys. Rev. C **82**, 027301 (2010).
- [40] E. Epelbaum, H. Krebs, and U.-G. Meissner, Eur. Phys. J. **A51**, 53 (2015).
- [41] M. Piarulli, L. Girlanda, R. Schiavilla, R. Navarro Perez, J.E. Amaro, and E. Ruiz Ariola, Phys. Rev. C **91**, 024003 (2015); M. Piarulli *et al.*, arXiv:1606.06335 [nucl-th].
- [42] S. Binder, A. Ekström, T. Papenbrock, K.A. Wendt, Phys. Rev. C **93**, 044002 (2016).
- [43] E. Friedman, Nucl. Phys. A **896**, 46 (2012); and references therein.
- [44] A. Trzcińska, J. Jastrzebski, P. Lubinski, F.J. Hartmann, R. Schmidt, T. von Egidy, and B. Klos, Phys. Rev. Lett. **87**, 082501 (2001).
- [45] W.R. Gibbs and J.-P. Dedonder, Phys. Rev. C **46**, 1825 (1992).
- [46] C. García-Recio, J. Nieves, E. Oset, Nucl. Phys. A **547**, 473 (1992).
- [47] M.B. Tsang, J.R. Stone, F. Camera, P. Danielewicz, S. Gandolfi, K. Hebeler, C.J. Horowitz, J. Lee, W.G. Lynch, Z. Kohley, R. Lemmon, P. Moller, T. Murakami, S. Riordan, X. Roca-Maza, F. Sammarruca, A.W. Steiner, I. Vidana, and S.J. Yennello, Phys. Rev. C **86**, 015803 (2012); and references therein.
- [48] T. Suzuki *et al.*, Phys. Rev. Lett. **75**, 3241 (1995).
- [49] T. Suzuki *et al.*, Nucl. Phys. A **630**, 661 (1998).
- [50] T. Suzuki *et al.*, Nucl. Phys. A **709**, 60 (2002).
- [51] G. Audi and A.H. Wapstra, Nucl. Phys. A **595**, 409 (1995).
- [52] F. Sammarruca and Y. Nosyk, Phys. Rev. C **94**, 044311 (2016).